Inhibitory control dysfunction in parkinsonian impulse control disorders

Garance M Meyer, Charlotte Spay, Alina Beliakova, Gabriel Gaugain, Gianni Pezzoli, Bénédicte Ballanger, Philippe Boulinguez, Roberto Cilia

OXFORD UNIVERSITY PRESS | Brain

Inhibitory control dysfunction in Parkinsonian Impulse Control Disorders

Journal:	*Brain*
Manuscript ID	BRAIN-2020-00564.R1
Manuscript Type:	Original Article
Date Submitted by the Author:	n/a
Complete List of Authors:	Meyer, Garance; Centre de Recherche en Neurosciences de Lyon; Université Claude Bernard Lyon 1 Spay, Charlotte; Centre de Recherche en Neurosciences de Lyon Beliakova, Alina; Centre de Recherche en Neurosciences de Lyon; Université Claude Bernard Lyon 1 Gaugin, Gabriel; Centre de Recherche en Neurosciences de Lyon Pezzoli, Gianni; Istituti Clinici di Perfezionamento, Parkinson Institute Ballanger, Benedicte; CNRS, Centre de Neuroscience Cognitive UMR 5229 Boulinguez, Philippe; Centre de Recherche en Neurosciences de Lyon; Université Claude Bernard Lyon 1 Cilia, Roberto; Fondazione IRCCS Istituto Neurologico Carlo Besta, Neurology
Subject category:	Movement disorders
To search keyword list, use whole or part words followed by an *:	Parkinson's disease: neurophysiology < MOVEMENT DISORDERS, Impulsivity and inhibition disorders < NEUROPSYCHIATRY, Beta oscillations < MOVEMENT DISORDERS, Motor control < MOVEMENT DISORDERS, Executive function < NEUROPSYCHIATRY

Inhibitory control dysfunction in Parkinsonian Impulse Control Disorders

Running title: Inhibitory control in PD-ICDs

Garance M. Meyer, MSc[1,2,3,4]*
Charlotte Spay, PhD[1,2,3,4]*
Alina Beliakova, MSc[1,2,3,4]
Gabriel Gaugain, MSc[1,2,3,4]
Gianni Pezzoli, MD[5,†]
Bénédicte Ballanger, PhD[1,2,3,4]
Philippe Boulinguez, PhD[1,2,3,4]**
Roberto Cilia, MD[6,†,]**

* *Co-first authors listed in alphabetical order*
** *Co-last authors listed in alphabetical order*

1. *Université de Lyon, F-69622, Lyon, France*
2. *Université Lyon 1, Villeurbanne, France*
3. *INSERM, U 1028, Lyon Neuroscience Research Center, Lyon, F-69000, France*
4. *CNRS, UMR 5292, Lyon Neuroscience Research Center, Lyon, F-69000, France*
5. *Fondazione Grigioni per il Morbo di Parkinson, Milan, Italy*
6. *Fondazione IRCCS Istituto Neurologico Carlo Besta, Milan, Italy*

† Previous affiliation: Parkinson Institute, ASST "Gaetano Pini-CTO", Milan, Italy

Corresponding Author:
Philippe Boulinguez
Centre de Recherche en Neurosciences de Lyon
95 boulevard Pinel, 69500 Bron, France
Phone: +33 4 72 13 89 78
Mail: philippe.boulinguez@univ-lyon1.fr

Word count: 5630

ABSTRACT

Impulse control disorders (ICDs) in Parkinson's disease (PD) have been associated with dysfunctions in the control of value- or reward-based responding (*choice impulsivity*) and abnormalities in mesocorticolimbic circuits. The hypothesis that dysfunctions in the control of response inhibition (*action impulsivity*) also play a role in PD-ICDs has recently been raised, but the underlying neural mechanisms have not been probed directly. We used high-resolution electroencephalography (EEG) recordings from 41 PD patients with and without ICDs to track the spectral and dynamical signatures of different mechanisms involved in inhibitory control in a simple visuomotor task involving no selection between competing responses and no reward to avoid potential confounds with reward-based decision. Behaviorally, PD patients with ICDs proved to be more impulsive than those without ICDs. This was associated with decreased beta activity in the precuneus and in a region of the medial frontal cortex centered on the supplementary motor area (SMA). The underlying dynamical patterns pinpointed dysfunction of proactive inhibitory control, an executive mechanism intended to gate motor responses in anticipation of stimulation in uncertain contexts. The alteration of the cortical drive of proactive response inhibition in PD-ICDs pinpoints the neglected role the precuneus might play in higher-order executive functions in coordination with the SMA, specifically for switching between executive settings. Clinical perspectives are discussed in the light of the non-dopaminergic basis of this function.

Keywords: Parkinson, impulsivity, inhibitory control, beta, precuneus.

1. INTRODUCTION

Impulse control disorders (ICDs) in Parkinson's disease (PD) including pathological gambling, hypersexuality, compulsive eating and compulsive shopping are a common side-effect of dopaminergic replacement therapy which has to date no satisfying therapeutic strategy. ICDs have been associated with decisional -also called cognitive or choice- impulsivity (Cilia and van Eimeren, 2011; Meyer *et al.*, 2019). Decisional impulsivity refers to dysfunctions in the control of value- or reward-based responding and is associated with dopamine agonist treatment and abnormalities in mesocorticolimbic circuits (Weintraub *et al.*, 2010; Cilia and van Eimeren, 2011; Aracil-Bolaños and Strafella, 2016; Hammes *et al.*, 2019; Meyer *et al.*, 2019). The hypothesis that dysfunctions in the control of motor response inhibition, i.e., motor or action impulsivity, also play a role in the etiology of PD-ICDs has received little interest, obtained little empirical support and has mostly been rejected (see Cilia and van Eimeren, 2011; Meyer *et al.*, 2019 for reviews). However, by reporting brain activity changes in inhibitory control regions, recent data have relaunched the hypothesis that ICDs might include a motor facet through the dysfunction of motor inhibition (van Eimeren *et al.*, 2010; Mosley *et al.*, 2019; Spay *et al.*, 2019; Paz-Alonso *et al.*, 2020). Yet, these studies only provide indirect evidence since the neural mechanisms underlying inhibitory control have not been isolated and addressed in an unconfounded manner. For instance, Spay and collaborators (2019) reported abnormal oscillatory activity in ICDs at rest in circuits supporting response inhibition (medial prefrontal cortex, rostral cingulate zone and supplementary motor area) but did not test directly response inhibition. Mosley and collaborators, too, did not directly probe response inhibition functions, but described a link between weaker structural connectivity of the response inhibition network and behavioral markers of pathological gambling (2019). van Eimeren and colleagues (2010) reported dopaminergic activity changes in PD gamblers with Positon Emission Tomography (PET)

during a card selection task in non-overlapping brain areas that have also been shown to be more or less directly involved in response inhibition (lateral orbitofrontal cortex, amygdala, external pallidum), but did not test directly response inhibition either. Paz-Alonso and colleagues (2020) used more sophisticated event-related and connectivity analyses with functional magnetic resonance imaging in a reward-based task. They reported in ICDs patients the involvement of various dysfunctions of a right-lateralized network of regions that are supposed to be associated with inhibitory control (subthalamic nucleus, ventral striatum, inferior frontal gyrus, insula). While there are many converging arguments in this study, there are however still potential confounds between reward-related and inhibitory-related activity since the slow event-related design was based on gambling-related cues. More generally, the large overlap that exists between the reward and inhibition networks as identified in the literature (e.g., ventral striatum, insula, STN, anterior cingulate, inferior frontal gyrus; Criaud and Boulinguez, 2013; Meyer *et al.*, 2019) prevents from concluding that inhibitory dysfunctions account for impulsive behavior when one of these regions shows reward-related activity changes (reverse inference issue, Poldrack, 2006).

All these observations allow raising the hypothesis that inhibitory dysfunctions could account for abnormal activity during reward processing or at rest, but do not demonstrate inhibitory dysfunctions in PD with ICDs with respect to PD without ICDs. To this aim, it is mandatory to ensure that the neural mechanisms involved in inhibitory control are probed directly irrespective of reward processing. Here, we capitalize on recent theoretical and methodological developments that now allow testing a range of possible mechanisms of response inhibition within a single experimental design while tracking their dynamical and spectral fingerprints directly at the electroencephalographic (EEG) source level in a simple visuomotor task involving no selection between competing responses and no reward.

2. MATERIAL & METHODS

A modified version of the Go/NoGo task was used to probe different types of inhibitory mechanisms that were not all tested in previous studies using Stop-Signal Task (SST), classical Go/NoGo Task or Continuous Performance Task (Criaud *et al.*, 2017). The present experiment is a follow-up study of (Spay *et al.*, 2019) using the same equipment and the same group of patients in a resting state study.

2.1. Participants

Twenty-seven PD patients (23 men, 4 women) with ICDs (ICDs+) and 22 PD patients (18 men, 4 women) without ICDs (ICDs-) were enrolled. ICDs+ had current ICDs despite previous treatment adaptation. All the patients underwent a 30-min semi-structured interview by experienced neuropsychologists to confirm the diagnosis of ICDs according to established diagnostic criteria (Siri *et al.*, 2015). Inclusion criteria were: age between 40 and 70 years old, with idiopathic PD according to MDS clinical diagnosis criteria (Postuma *et al.*, 2015), benefiting from a stable antiparkinsonian drug therapy for at least 2 months. Exclusion criteria were: dementia (MMSE < 26), other neurologic or psychiatric disease, pharmacological treatment with cerebral or psychic impact, substance abuse according to the criteria DSM-IV-TR (except tobacco smoking). Patients were tested in the morning in the ON-state, on their usual medication. Clinical and neuropsychological assessment included the Mini Mental State Examination (MMSE), the Frontal Assessment Battery (FAB), the Minnesota Impulsive Disorders Interview (MIDI) and the Questionnaire for Impulsive-Compulsive Disorders in Parkinson Disease (QUIP) to assess ICDs, the Barratt Impulsiveness Scale (BIS-11), the Beck Depression Inventory (BDI), the UPDRS-III (Unified Parkinson's Disease Rating Scale part III), the evaluation of the presence of motor fluctuations (sum of items 36 to 39 of the UPDRS part IV different from 0) and the evaluation of Hoehn & Yahr (H&Y) stage. Data from 3 participants had to be discarded following inabilities to perform the task while data from 7

participants had to be discarded following technical issues during data acquisition. Ultimately, two groups of 22 ICDs+ (21 men, 1 woman) and 19 ICDs- (17 men, 2 women) patients of similar age, disease duration, levodopa equivalent daily dose (LEDD) and Unified PD Rating Scale (UPDRS) part III were included. The main demographic and clinical characteristics of the patients are displayed in Table 1.

This study was performed in agreement with the principles of the Declaration of Helsinki and the protocol was approved by the local Ethical Committee of the Parkinson Institute, Milan, Italy. Written informed consent was obtained from all the patients before the study.

2.2. Behavioral task

Principle:

Patients performed a simplified Go/NoGo task developed by our group (Criaud and Boulinguez, 2013; Albares *et al.*, 2015; Criaud *et al.*, 2017) (Figure 1A). In this task, different inhibitory mechanisms might be involved (Figure 1B). Action restraint can first be achieved through proactive mechanisms. Proactive inhibition operates as a gating process implemented in anticipation of stimulation, which suppresses movement initiation function when the context is uncertain (Jaffard *et al.*, 2007, 2008; Criaud *et al.*, 2017). Here, context uncertainty has been manipulated in different blocks of trials mixing up or not target stimuli requiring a response (Go) and non-target stimuli requiring to refrain from reacting (NoGo). In mixed-blocks, equiprobable Go and NoGo trials could be presented (uncertain context). In pure-blocks (control condition), no NoGo stimuli could be presented (Go_control trials only), meaning that action restraint was no longer required since there was no uncertainty about the nature of the upcoming event (contrast 1, [Go - Go_control]). Response inhibition can also be achieved by means of late, reactive mechanisms specifically triggered by the stimulus subjects must refrain from reacting to, but not by the Go stimulus subjects must react to (Rubia *et al.*,

2001; Swick *et al.*, 2011). These selective reactive mechanisms have been assessed by contrasting NoGo and Go trials (contrast 2). Finally, response inhibition might also be achieved by means of reactive mechanisms triggered non-selectively and automatically by any stimulus (either Go or NoGo) when the context is uncertain, but not when there is no need to refrain from reacting. This form of automatic inhibition is intended to counteract automatic responses (affordances) to stimuli that have not yet been fully identified (Jasinska, 2013; Albares *et al.*, 2014) or when time is needed to settle on the decision to act or the decision to choose between actions (Frank, 2006; Wiecki and Frank, 2013). Since this function is context dependent and requires an executive setting (Chiu and Aron, 2014), it has been assessed here by means of contrast 3 ([(Go+NoGo) - Go_control]) (Figure 1).

In this task, the rate of erroneous responses to NoGo stimuli (commissions) is indicative of impulsive behavior. Since non-selective, context-dependent mechanisms of response inhibition apply to all stimuli, long latency voluntary response are usually provided after the initial response to a Go stimulus has been suppressed. Therefore, in this task reaction time (RT) is indicative of the level of proactive inhibition and/or the involvement of non-selective reactive inhibition.

Apparatus and procedure:

A panel equipped with light-emitting diodes (LEDs – Ø5mm, 8800mcd) was used to present the visual stimuli. One LED was placed in the center of the panel and set at the subject's eye level. It served as a fixation point for the eyes and indicated the beginning of the trial and the type of block (green –pure-block- or red –mixed-block-). The target stimulus (Go) was composed of eight other LEDs forming a green diamond. The NoGo stimulus was composed of eight LEDs forming a green cross. A feedback stimulus was composed of four LEDs forming a square (green –correct response- or red –incorrect response-). Go, NoGo and feedback stimuli were centered on the fixation point and occupied 3.44° of visual angle. Stimuli were presented, and data were acquired using a real time acquisition system (ADwin

Pro, Keithley Instruments, Cleveland, OH) controlled by MatlabTM software (MATLAB, RRID:SCR_001622).

The participants were seated in a darkened room in front of a screen placed 50cm from their eyes. The appearance of the fixation point indicated the beginning of a trial and lasted until the presentation of the stimulus. Pre-stimulus delays (time between the beginning of a trial and stimulus presentation) varied randomly from two to four seconds in steps of 500 ms. The stimuli (Go or NoGo) were presented for 50 ms. Participants were asked to react as fast as possible to target presentation by pressing a button with their right index within one second timing. A feedback was given to the subject to indicate if the response was correct (green square) or not (red square). The inter-trial interval was up to the subject who had to press a button with the left index to go on the next trial. This procedure allowed participants to take as many rest-breaks as necessary. Participants were instructed to comply with a maximum error rate (commissions and omissions) of 20% of all trials to ensure a good understanding of the task. A block design was used to test the two conditions separately. Four blocks of trials (two mixed-blocks, two pure-blocks) were presented in a counterbalanced order between participants (ABBA or BAAB). Pure-blocks were composed of 35 Go_control trials each, for a total of 70 Go_control trials per subject. Mixed-blocks were composed of 35 Go trials and 35 NoGo trials each, randomly presented, for a total of 70 Go trials and 70 NoGo trials per subject. Participants were trained with the task before starting the experimental sessions (2 pure-blocks, 1 mixed-block).

2.3. Electroencephalographic recordings

Principle:

We used high-density EEG for the strong functional discrimination power it provides through spectral analyses, as frequency-specific activity provides markers of cognitive-

specific mechanisms. Of particular interest is the possibility to disentangle the active inhibitory mechanisms that gate information processing (active inhibition) from top-down signaling and communication between control areas (cortical drive), respectively indexed by alpha and beta oscillations (Engel and Fries, 2010; Jensen and Mazaheri, 2010; Kilavik *et al.*, 2013; Albares *et al.*, 2015; Liebrand *et al.*, 2018). Importantly, the spectral dynamics of the different mechanisms possibly involved in inhibitory control (Figure 1B) has been assessed directly at the source level, thanks to procedures based on group blind source separation (gBSS) issued from recent methodological developments (Lio and Boulinguez, 2013, 2018; Albares *et al.*, 2015; e.g. see Albares *et al.*, 2014 for analyses of reactive inhibition and Spay *et al.*, 2018 for analyses of proactive inhibition). In order to investigate all cortical networks potentially involved in impulsivity related to ICDs, we performed whole-brain/whole spectrum analyses replicated from our previous work in healthy subjects (ibid). Figure 2 presents an overview of the processing pipeline.

Apparatus and procedure:

The Biosemi™ ActiveTwo Mk2 system (31.25nV resolution) was used to record EEG data from 128 electrodes mounted in an elastic cap at Biosemi™ ABC system standard locations. Six additional external electrodes were added: four temporal electrodes (Biosemi spherical coordinates: Phi -103.5 Theta -18 -36, and Phi 103.5 Theta 18 36), and two electrodes attached to the outer canthi of the left and right eyes (Phi 103.5 -103.5 Theta 81 -81). The CMS active electrode and the DRL passive electrode of the ActiveTwo system were used instead of classical ground electrodes of conventional systems (these two electrodes form a feedback loop driving the average potential of the subject - the Common Mode voltage - as close as possible to the analogue-to-digital reference voltage in the AD-box). All electrode offsets were kept below 20mV. EEG data were recorded at a sampling rate of 4096Hz.

Data preprocessing:

Data were down-sampled at 2048 Hz, filtered (High-pass 0.5-1 Hz; Low-pass 46-48 Hz; Attenuation 80 dB) and set to average reference. Then, data were epoched from 1500 ms before stimulus onset to 1000 ms after stimulus onset. Two steps were implemented to reject artifacts. For each subject and each block of trials (pure-block, mixed-block), corrupted epochs and artifacts (blinks, eye movements, ballistocardiac noise and other electrical noises) were detected and rejected using a first independent component analysis (ICA) / blind source separation (BSS) (UWSOBI, 300 times delays; Yeredor, 2000) and the EEGLAB toolbox (Delorme and Makeig, 2004). Then, in a second step, an automatic rejection procedure for outlier epochs has been applied. For each epoch, the Frobenius norm between the epoch's covariance matrix and the dataset's mean covariance matrix was calculated and, for each dataset, the 5% of the epochs deemed as outliers according to this metric have been rejected.

Group Blind Source Separation (gBSS):

We applied gBSS for the detection of task related sources. This approach offers a straightforward and computationally tractable solution to the problem of multi-subject analysis by creating aggregate data containing observations from all participants. By providing a single estimation of the mixing and the demixing matrices for the whole group, gBSS allows direct estimation of the components that are consistently expressed in the population (Eichele *et al.*, 2011) and, hence, more efficient source separation and localization of these components (Lio and Boulinguez, 2013). A potential benefit of this method is a better sensitivity for the detection of critical sources that are often occulted by the most energetic phenomena (Sutherland and Tang, 2006). We employed UWSOBI, a Second Order Statics based gBSS algorithm based on the approximate joint diagonalization of lagged-covariance matrices since this method is robust with respect to anatomo-functional inter-subjects variability and can separate group specific uncorrelated sources with non-proportional power-

spectra without deleterious prior dimension reduction (Lio and Boulinguez, 2018). This method is especially convenient here because it separates the sources based on their spectral signatures (Albares *et al.*, 2015). Two hundred lagged-covariance matrices with time delays from 0/2048s to 200/2048s were calculated on each epoch. Then, lagged-covariance matrices were averaged across the dataset epochs, and then across patients, so that 200 lagged-covariance matrices were approximately joint-diagonalized with the UWEDGE algorithm (Tichavsky and Yeredor, 2009), leading to the identification of 134 ICs. Thanks to this averaging procedure, inter-epochs and inter-subjects variability was reduced without impeding the capacity to identify sources with spectral modifications between groups later on (e.g., Ramoser *et al.*, 2000; Congedo *et al.*, 2008). The components were sorted by percent of explained variance. All components explaining more than 1% of the overall variance of the signal were selected for further analyses.

Spectral decomposition:

To get all recordable sources underlying inhibitory control, we performed blind spectral analyses without a priori about anatomical sources or frequency bands. We assessed trial-by-trial modulations for all ICs explaining more than 1% of overall variance in the delta/theta (1.5-7.5 Hz), alpha (7.5- 13.5 Hz), beta 1-2 (13.5-19.5 Hz), beta 3 (19.5-30.5 Hz), and low gamma (30.5-44.5 Hz) bands. Spectral decomposition was based on six Elliptic Infinite Impulse Response (IIR) bandpass filters designed with the MatlabTM signal processing toolbox to get optimal time/frequency resolution. Relatively large pass band widths were set to get optimal estimation of the temporal dynamics of the frequency bands of interest at the single trial level. Detailed specification of the filters can be found in (Albares et al., 2014). Single trial power modulation was then estimated for each source and each frequency band thanks to the Hilbert transform: First, each trial was filtered with the corresponding filter in both forward and reverse directions to insure zero-phase distortion.

Second, the complex analytic signal was derived by the Hilbert transform (MatlabTM hilbert function). Third, the instantaneous amplitude envelope of the signal was computed by taking the absolute magnitude of the complex waveform. The time window under scrutiny was restricted to 500 ms pre-stimulus to 800 ms post-stimulus to avoid edge effects/transient responses of digital filters. Finally, for visualization only, a trial moving average smoothing was applied (windows length: 400 trials).

Statistical matching procedure:

We used the following rationale to identify the sources potentially involved in inhibitory control: If the mean power of the pre-stimulus period [-500; 0 ms] was significantly larger than the mean power of the period preceding reaction time [RT-100 ms; RT] for Go trials (Go-induced desynchronization), then this source/frequency band was considered as playing a possible role in proactive inhibition and was selected for further group analyses. If the mean power of the post-stimulus period [0; 300 ms] was significantly different for Go+NoGo than for Go_control trials, and if the mean power of the post-stimulus period [0; 300ms] was significantly larger than the mean power of the pre-stimulus period [-500; 0 ms], then the corresponding source/frequency band was considered as playing a possible role in reactive non-selective inhibition, and was selected for further group analyses. If the mean power of the post-stimulus periods [0; 150 ms], [150; 250 ms] or [250; 350 ms] was significantly larger for NoGo than for Go trials, then the corresponding source/frequency band was considered as playing a possible role in reactive selective inhibition, and was selected for further group analyses. These testing procedures were applied to the control group data only (ICDs-) and used Wilcoxon-Mann-Whitney and Wilcoxon signed-rank tests.

Group analyses:

Deconcatenation for between-subject analyses has been performed to have access to inter-individual variability for further statistical analyses. The consistent ICs revealed at the

group level were used as filters for these analyses. This step-back to the individual level allows individual data normalization by calculating the mean relative power within each frequency band with respect to the total power of the EEG signal (whole spectrum) for each single source/subject.

Mean relative power spectral density (PSD) has been estimated for each selected source by means of short-time Fourier transforms (MatlabTM signal processing toolbox spectrogram), with a window width of 800 samples and an overlap of 799 in the 1-45 Hz frequency range:

$$\forall f \in [1,45],\ \ PSD_{rel}(SSi,f) = \frac{PSD_{abs}(SSi,f)}{\sum_{f_k=1}^{45} PSD_{abs}(SSi,f_k)}$$

Where SSi is the selected source n°i.

Source localization:

When relevant, localization was estimated by means of the sLoreta software (Pascual-Marqui, 2002) and a head model obtained by applying the BEM method to the MNI152 template (Mazziotta *et al.*, 2001). The 3D solution space was restricted to cortical gray matter and was partitioned into 6239 voxels with a spatial resolution of 5mm. Then, the sLoreta solution of the inverse problem was computed using an amount of Tikhonov regularization optimized for an estimated Signal/Noise Ratio of 100.

2.4. Statistical analyses

Behavioral variables:

Commissions (erroneous responses to NoGo stimuli) are usually considered as the main behavioral marker of impulsivity and inhibitory dysfunction in PD (e.g., Ballanger *et al.*, 2009). The rate of commissions was assessed only in the mixed-block condition where erroneous responses to NoGo stimuli are possible. Normality and homoscedasticity were controlled using respectively Lillefors test and Fisher test. Between subjects' analyses of

mean percentage of commissions were performed after ArcSine transforms. The group effect (ICDs+ vs. ICDs-) was tested by means of a one-sided t test for independent samples. Reaction time is known to pinpoint the level of action restraint (e.g., Chiu and Aron, 2014). In the Go_control condition, when no inhibition is required, automatic motor activations usually give rise to fast responses. Conversely, when action restraint is required in uncertain contexts, proactive inhibition and/or reactive non-selective inhibition prevent fast automatic responses. Volitional responses can be provided only after the Go stimulus has been identified and the executive inhibitory set has been released. This generates long latency responses (Jaffard *et al.*, 2007, 2008; Boulinguez *et al.*, 2008; Criaud *et al.*, 2012, 2017). Accordingly, we assessed the difference in RT between Go and Go_control conditions (delta RT), which is known to index the level of non-selective inhibition (the context-dependent inhibitory set, Chiu and Aron, 2014). Normality and homoscedasticity were controlled using respectively Lillefors test and Fisher test. The group effect (ICDs+ vs. ICDs-) was tested by means of a one-sided t test for independent samples.

EEG variables:

For each selected source/frequency band showing relevant proactive activity, mean relative PSD during the pre-stimulus period [-500; 0 ms] was assessed by means of a 2 groups (ICDs+ vs. ICDs-) x 2 conditions (Go+NoGo vs. Go_control) ANOVA. These analyses were performed with R (R Core Team, 2014). Post hoc tests used the R package emmeans. P values under 0.05 were considered significant. No similar analyses have been applied to reactive non-selective or reactive selective activities as the statistical matching procedure returned no ICs/frequency bands showing significant modulation (see Results section).

2.5. Complementary analyses

In order to better understand the role of the dysfunctional components within the global sensorimotor network identified in the previous step, we performed complementary analyses to estimate the directionality and lag between the respective brain activities. Since the spectral dynamics of the dysfunctional neural sources identified in the previous step present patterns consistent with proactive inhibition, we tested the directionality of the relationship between the desynchronizations that occur just before the motor onset. Specifically, we used cross-correlation of instantaneous amplitudes estimated via the Hilbert transform to measure lagged-consistency between the desynchronization patterns of the different sources and infer the direction of functional connectivity. This method was privileged over algorithms relying on the concept of Granger causality (which are the standard method to assess this kind of relationships between time series; Astolfi *et al.*, 2007) because it circumvents the bias related to differences in signal-to-noise ratios between sources (Adhikari *et al.*, 2010). Indeed, when such differences are observed (as it is expected to be the case in this study), the algorithms based on Granger causality interpret the related asymmetries as directions of information flow, leading to false estimations of the directional connectivity (Nolte *et al.*, 2008; Adhikari *et al.*, 2010; Haufe *et al.*, 2013; Bastos and Schoffelen, 2015).

The technique was adapted to focus on task-related changes in cross-correlations, and avoid potential confounds with volume conduction effects leading to spurious false positives (Schoffelen and Gross, 2009; Bastos and Schoffelen, 2015). More precisely, each connection was evaluated with the following procedure: First, the instantaneous amplitude time course of each trial was split in one pre-stimulus baseline epoch (from 1000ms to 100ms before the stimulation onset) and one post-stimulus epoch of interest (-100ms; 800ms). Second, for each subject, all epochs were averaged and the resulting average time-course was Z-transformed to reduce the non-stationarity of the signal. Then, cross-correlation limited by 200ms between

each pair of components was estimated on an individual basis. Third, each lag was tested using the Wilcoxon-Mann-Whitney test, tracking significant increases in cross-correlations in the post-stimulus period relative to spontaneous cross-correlations in the baseline. Connections showing a lagged correlation with a p-value<0.05 (Bonferroni corrected for all tested connections) were deemed significant. For each pair of source/frequency band combinations of interest, the most significant cross-correlation was considered as the most probable connection. If the same minimal p-value was observed for two or more different lags, the smallest lag was selected.

2.6. Data availability

The data will be made available upon request to the corresponding author.

3. RESULTS

3.1. Behavioral variables

More commission errors were observed for ICDs+ than for ICDs- (17.1% vs 7.0%, T(39)=3.28, p=0.007). Shorter delta RT was observed for ICDs+ than for ICDs- (165.47 vs 193.54, T(39)=-1.69, p=0.048). Control analyses indicated that experiencing motor fluctuations or not (157.63 vs 181.12, W=40, p=0.41) as well as having single ICD or multiple ICDs (163.94 vs 166.50, W=66, p=0.72) did not significantly influenced the behavior (delta RT) of ICDs+.

3.2. EEG variables

Detailed EEG results are displayed in Table 2.

Network involved in inhibitory control as assessed in ICDs- patients

The gBSS revealed a network comprising visual, frontal and parietal areas (14 ICs explaining more than 1% of overall variance; Figure 3, Table 2). The statistical matching procedure revealed 47 IC/frequency band combinations with dynamics consistent with proactive inhibition (i.e., Go-induced desynchronization, Table 2). Fourteen ICs/frequency bands showed stimulus-induced synchronization patterns. However, none revealed significant differences between NoGo+Go and Go_control trials consistent with reactive non-selective inhibition, nor significant differences between NoGo and Go trials consistent with reactive selective inhibition.

Dysfunctional sources in ICDs+ patients

Among the 47 IC/frequency band combinations showing activity consistent with proactive inhibition, seven showed significant Group by Condition interaction (Table 2). Planned post-hoc comparisons were applied to track the impact of belonging to one or the other group on the ability to modulate as expected proactive activity according to the context (i.e., more power for NoGo+Go trials than for Go_Control trials). Only three IC/frequency band combinations reported a consistent pattern in ICDs- but a different one in ICDs+: ICs #4 and #6 centered on the precuneus (beta 1-2 activity) and IC #8 in the medial frontal cortex (centered on the supplementary motor area -SMA-; beta 3 activity) (Table 2). For these three ICs, ICDs+ showed either no significant difference between conditions (ICs#4,6), or an opposite pattern (IC#8) (Figure 4, Table 2).

Position of the dysfunctional sources within the functional fronto-parietal network

Directionality analyses reported that desynchronization of parietal IC#6 precedes stimulus-induced modulations of parietal IC#4 by 8ms ($p<.0001$) and frontal IC#8 by 17ms ($p<.0001$). Desynchronization of IC#8 was also found to precede stimulus-induced modulations of parietal IC#4 by 58ms ($p<.0001$). A detailed report of lag statistics between

these three dysfunctional sources and all other frontal and parietal sources of the network involved in inhibitory control as assessed in ICDs- patients (see above) is available in Supplementary Table 1. The most notable result is that frontal IC#8 leads all other frontal sources. Figure 5 presents a synthesis of this connectivity analysis.

4. DISCUSSION

In a simple task involving no selection between multiple competing responses, no reward, and no delay discounting, the increased commission error rate in PD patients with ICDs provides global evidence for impaired motor response inhibition. The decrease in delta RT to Go stimuli also suggests that less motor inhibition is implemented in uncertain contexts (Wardak *et al.*, 2012; Chiu and Aron, 2014; Criaud *et al.*, 2017). In other words, ICDs in PD might partly be due to action impulsivity, not just choice impulsivity. This outcome provides empirical support to former isolated hypotheses (van Eimeren *et al.*, 2010; Cilia and van Eimeren, 2011; Brevers *et al.*, 2012; Mosley *et al.*, 2019; Spay *et al.*, 2019; Paz-Alonso *et al.*, 2020).

Consistent with behavioral results, electrophysiological analyses pinpoint dysfunctions of proactive response inhibition as seen in reduced pre-stimulus beta activity in the SMA and the precuneus when action restraint is required (Figure 4). The abnormal activity observed in the SMA in PD-ICDs is highly consistent with its well-known role in executive control and response inhibition (Rubia *et al.*, 2001; Isoda and Hikosaka, 2007; Sumner *et al.*, 2007; Nachev *et al.*, 2008; Swick *et al.*, 2011). It is also reminiscent of former connectivity study emphasizing the implication of SMA abnormalities in ICDs through structural disconnections with motor and associative regions of the basal ganglia (Mosley *et al.*, 2019). By contrast, the identification of the precuneus as a source of dysfunction of motor inhibition may, at a first glance, come as a surprise regarding the minor role the precuneus is usually supposed to play

in higher-order cognitive functions (but see Cavanna and Trimble, 2006 for a review of some contradictory evidence). However, the present result is in line with the observation that the precuneus is involved, although in a very unclear way, in the preparation and execution of spatially guided behaviors in association with the sensorimotor fronto-parietal network (Zhang and Li, 2012), and in the control of response inhibition (Barber and Carter, 2005; Criaud *et al.*, 2017; Lemire-Rodger *et al.*, 2019) in healthy subjects. It is also consistent with former observations that impaired activity in the precuneus is associated with response control disorders. More specifically, abnormally high proactive activity in the precuneus has been related to exaggerated inhibitory control in PD (Criaud *et al.*, 2016) while, conversely, decreased activity in the precuneus has been related to impulsivity in PD patients (Ballanger *et al.*, 2009).

The fact that neural correlates of ICDs are observed in the precuneus and in the SMA in the beta band suggests that the origin of the problem is not purely motor. Indeed, in the context of the present study, beta oscillations are likely to index top-down signaling between sensorimotor and non-sensorimotor areas (Engel and Fries, 2010; Albares *et al.*, 2015). As such, the alteration of the cortical drive of proactive motor inhibition observed in ICDs at the level of the SMA and the precuneus might rather index an impairment of the executive control of motor inhibitory networks, and more particularly in the ability to switch between executive sets for which both are known to play a major role (Lemire-Rodger *et al.*, 2019).

Although the exact role played by the SMA and precuneus cannot be precisely identified in the present study, connectivity analyses reveal a prominent position within the fronto-parietal network involved in response control (Figure 3, Figure 5). In particular, one of the two dysfunctional beta sources in the precuneus desynchronizes early within the cascade of events induced by stimulus presentation in the overall sensorimotor network. This source is likely to lead the subsequent desynchronization of the beta SMA dysfunctional source (Figure

5A), which itself has a leading role in the cascade of event-related desynchronizations observed in the frontal areas of the network (Figure 5C). In other words, according to the hypothetical role of beta activity in top-down signaling (Engel and Fries, 2010; Albares *et al.*, 2015), the precuneus may act as a trigger in the frontal control processes, and its dysfunction may result in an impaired capacity to implement inhibitory control in the motor system in anticipation of stimulation. This observation is reminiscent of previous reports of abnormal connectivity between the precuneus and the motor system in PD patients (Thibes *et al.*, 2017). However, the complex pattern of interactions between the dysfunctional sources in ICDs and the rest of the sensorimotor system can still not be fully inferred from the present results.

In conclusion, our findings support the hypothesis that the specific impairment of PD patients with ICDs with respect to PD patients without ICDs would stem in the weaker ability of the former to sustain and switch between executive settings. However, there remain important caveats that must be borne in mind when interpreting these results. First, it cannot be concluded that the frontal mechanisms that directly suppress motor activation are more impaired in PD patients with ICDs than in PD patients without ICDs. Second, the present data do not mean that there are no other specific frontal dysfunctions in PD-ICDs with respect to PD without ICDs (Mosley *et al.*, 2019). In the present experiment, which does not confound reward processing and inhibitory control, this would rather mean that the frontal dysfunctions often observed in PD-ICDs (in particular in cingulate and orbitofrontal cortices, van Eimeren *et al.*, 2010; Santangelo *et al.*, 2019) might not be directly related to motor response inhibition *per se*. This does not mean, either, that no other brain region can account for the behavioral differences observed between ICDs+ and ICDs-. Given the limited capacity of EEG to identify deep sources, and the acknowledged role of the basal ganglia in both proactive and reactive control inferred from direct electrophysiological recordings (e.g., Benis *et al.*, 2014), it is most likely that abnormal beta activity in the precuneus and in the SMA are not the

unique sources of inhibitory dysfunction in PD-ICDs. In addition, the task used in this study certainly makes fewer demands on reactive mechanisms of inhibition (Criaud and Boulinguez, 2013) and likely ignores other cortical sources of inhibitory dysfunction in PD-ICDs.

Notwithstanding these limitations, the evidence that dysfunctions of action control play a role in ICDs might open the door to new research avenues and support possible treatment strategies including complementary non-dopaminergic medication. Indeed, DA medication would mainly influence the neural network underlying impulsive choices but not the neural network underlying impulsive action (Antonelli *et al.*, 2014). Importantly, previous work on the neural and neurochemical bases of inhibitory control has identified the key role of both the noradrenergic (NA) and the serotoninergic (5HT) systems (Eagle *et al.*, 2008; Robbins and Arnsten, 2009; Ye *et al.*, 2014). In light of former studies in PD (Kehagia *et al.*, 2014; Rae *et al.*, 2016; Spay *et al.*, 2018), greater emphasis might especially be placed on noradrenergic therapies in future clinical trials for the treatment of ICDs. However, the present results suggest that the diverse forms of response inhibition might be differently affected in ICDs. Thus, as inspired by former psychiatry research (Eagle *et al.*, 2008; Dalley and Robbins, 2017), fractionating impulsivity into distinct neural mechanisms might prove necessary to identify and treat specifically various possible forms of impulsive behavior in PD-ICDs that remain to be elucidated (Meyer *et al.*, 2019).

ACKNOWLEDGEMENTS

The authors are thankful to Francesca Natuzzi, Francesco Turco and Chiara Siri, who helped for organizing the project, and are also thankful to Mauro Schiavella and Matteo Pelagatti from the University of Milan-Bicocca who substantially contributed to the build-up of local capacity. RC thanks the "Fondazione Grigioni per il Morbo di Parkinson", Milan (Italy) for supporting clinical research.

FUNDING

This work was supported by a grant ANR ANR-16-CE37-0007-03 to Philippe Boulinguez and a grant PALSE 2016 to Charlotte Spay.

COMPETING INTERESTS

None.

REFERENCES

Adhikari A, Sigurdsson T, Topiwala MA, Gordon JA. Cross-correlation of instantaneous amplitudes of field potential oscillations: a straightforward method to estimate the directionality and lag between brain areas. J Neurosci Methods 2010; 191: 191–200.

Albares M, Lio G, Boulinguez P. Tracking markers of response inhibition in electroencephalographic data: why should we and how can we go beyond the N2 component? Reviews in the Neurosciences 2015; 26: 461–478.

Albares M, Lio G, Criaud M, Anton J-L, Desmurget M, Boulinguez P. The dorsal medial frontal cortex mediates automatic motor inhibition in uncertain contexts: evidence from combined fMRI and EEG studies. Hum Brain Mapp 2014; 35: 5517–31.

Antonelli F, Ko JH, Miyasaki J, Lang AE, Houle S, Valzania F, et al. Dopamine-agonists and impulsivity in Parkinson's disease: impulsive choices vs. impulsive actions. Hum Brain Mapp 2014; 35: 2499–506.

Aracil-Bolaños I, Strafella AP. Molecular imaging and neural networks in impulse control disorders in Parkinson's disease. Parkinsonism Relat Disord 2016; 22 Suppl 1: S101-105.

Astolfi L, Cincotti F, Mattia D, Marciani MG, Baccala LA, de Vico Fallani F, et al. Comparison of different cortical connectivity estimators for high-resolution EEG recordings. Hum Brain Mapp 2007; 28: 143–57.

Ballanger B, van Eimeren T, Moro E, Lozano AM, Hamani C, Boulinguez P, et al. Stimulation of the subthalamic nucleus and impulsivity: release your horses. Ann Neurol 2009; 66: 817–24.

Barber AD, Carter CS. Cognitive control involved in overcoming prepotent response tendencies and switching between tasks. Cereb Cortex 2005; 15: 899–912.

Bastos AM, Schoffelen J-M. A Tutorial Review of Functional Connectivity Analysis Methods and Their Interpretational Pitfalls. Front Syst Neurosci 2015; 9: 175.

Benis D, David O, Lachaux J-P, Seigneuret E, Krack P, Fraix V, et al. Subthalamic nucleus activity dissociates proactive and reactive inhibition in patients with Parkinson's disease. Neuroimage 2014; 91: 273–81.

Boulinguez P, Jaffard M, Granjon L, Benraiss A. Warning signals induce automatic EMG activations and proactive volitional inhibition: evidence from analysis of error distribution in simple RT. J Neurophysiol 2008; 99: 1572–8.

Brevers D, Cleeremans A, Verbruggen F, Bechara A, Kornreich C, Verbanck P, et al. Impulsive action but not impulsive choice determines problem gambling severity. PLoS ONE 2012; 7: e50647.

Cavanna AE, Trimble MR. The precuneus: a review of its functional anatomy and behavioural correlates. Brain 2006; 129: 564–83.

Chiu Y-C, Aron AR. Unconsciously triggered response inhibition requires an executive setting. J Exp Psychol Gen 2014; 143: 56–61.

Cilia R, van Eimeren T. Impulse control disorders in Parkinson's disease: seeking a roadmap toward a better understanding. Brain Struct Funct 2011; 216: 289–99.

Congedo M, Gouy-Pailler C, Jutten C. On the blind source separation of human electroencephalogram by approximate joint diagonalization of second order statistics. Clin Neurophysiol 2008; 119: 2677–86.

Criaud M, Boulinguez P. Have we been asking the right questions when assessing response inhibition in go/no-go tasks with fMRI? A meta-analysis and critical review. Neurosci Biobehav Rev 2013; 37: 11–23.

Criaud M, Longcamp M, Anton J-L, Nazarian B, Roth M, Sescousse G, et al. Testing the physiological plausibility of conflicting psychological models of response inhibition: a forward inference fMRI study. Behav Brain Res 2017; 333: 192–202.

Criaud M, Poisson A, Thobois S, Metereau E, Redouté J, Ibarrola D, et al. Slowness in Movement Initiation is Associated with Proactive Inhibitory Network Dysfunction in Parkinson's Disease. J Parkinsons Dis 2016; 6: 433–40.

Criaud M, Wardak C, Ben Hamed S, Ballanger B, Boulinguez P. Proactive inhibitory control of response as the default state of executive control. Front Psychol 2012; 3: 59.

Dalley JW, Robbins TW. Fractionating impulsivity: neuropsychiatric implications. Nat Rev Neurosci 2017; 18: 158–71.

Delorme A, Makeig S. EEGLAB: an open source toolbox for analysis of single-trial EEG dynamics including independent component analysis. J Neurosci Methods 2004; 134: 9–21.

Eagle DM, Bari A, Robbins TW. The neuropsychopharmacology of action inhibition: cross-species translation of the stop-signal and go/no-go tasks. Psychopharmacology (Berl) 2008; 199: 439–56.

Eichele T, Rachakonda S, Brakedal B, Eikeland R, Calhoun VD. EEGIFT: group independent component analysis for event-related EEG data. Comput Intell Neurosci 2011; 2011: 129365.

van Eimeren T, Pellecchia G, Cilia R, Ballanger B, Steeves TDL, Houle S, et al. Drug-induced deactivation of inhibitory networks predicts pathological gambling in PD. Neurology 2010; 75: 1711–6.

Engel AK, Fries P. Beta-band oscillations--signalling the status quo? Curr Opin Neurobiol 2010; 20: 156–65.

Frank MJ. Hold your horses: A dynamic computational role for the subthalamic nucleus in decision making. Neural Networks 2006; 19: 1120–36.

Hammes J, Theis H, Giehl K, Hoenig MC, Greuel A, Tittgemeyer M, et al. Dopamine metabolism of the nucleus accumbens and fronto-striatal connectivity modulate impulse control. Brain 2019; 142: 733–43.

Haufe S, Nikulin VV, Müller K-R, Nolte G. A critical assessment of connectivity measures for EEG data: a simulation study. Neuroimage 2013; 64: 120–33.

Isoda M, Hikosaka O. Switching from automatic to controlled action by monkey medial frontal cortex. Nat Neurosci 2007; 10: 240–8.

Jaffard M, Benraiss A, Longcamp M, Velay J-L, Boulinguez P. Cueing method biases in visual detection studies. Brain Res 2007; 1179: 106–18.

Jaffard M, Longcamp M, Velay J-L, Anton J-L, Roth M, Nazarian B, et al. Proactive inhibitory control of movement assessed by event-related fMRI. Neuroimage 2008; 42: 1196–206.

Jasinska AJ. Automatic inhibition and habitual control: alternative views in neuroscience research on response inhibition and inhibitory control. Front Behav Neurosci 2013; 7: 25.

Jensen O, Mazaheri A. Shaping functional architecture by oscillatory alpha activity: gating by inhibition. Front Hum Neurosci 2010; 4: 186.

Kehagia AA, Housden CR, Regenthal R, Barker RA, Müller U, Rowe J, et al. Targeting impulsivity in Parkinson's disease using atomoxetine. Brain 2014; 137: 1986–97.

Kilavik BE, Zaepffel M, Brovelli A, MacKay WA, Riehle A. The ups and downs of β oscillations in sensorimotor cortex. Exp Neurol 2013; 245: 15–26.

Lemire-Rodger S, Lam J, Viviano JD, Stevens WD, Spreng RN, Turner GR. Inhibit, switch, and update: A within-subject fMRI investigation of executive control. Neuropsychologia 2019; 132: 107134.

Liebrand M, Kristek J, Tzvi E, Krämer UM. Ready for change: Oscillatory mechanisms of proactive motor control. PLoS ONE 2018; 13: e0196855.

Lio G, Boulinguez P. Greater robustness of second order statistics than higher order statistics algorithms to distortions of the mixing matrix in blind source separation of human EEG: Implications for single-subject and group analyses. NeuroImage 2013; 67: 137–52.

Lio G, Boulinguez P. How Does Sensor-Space Group Blind Source Separation Face Inter-individual Neuroanatomical Variability? Insights from a Simulation Study Based on the PALS-B12 Atlas. Brain Topogr 2018; 31: 62–75.

Mazziotta J, Toga A, Evans A, Fox P, Lancaster J, Zilles K, et al. A probabilistic atlas and reference system for the human brain: International Consortium for Brain Mapping (ICBM). Philos Trans R Soc Lond B Biol Sci 2001; 356: 1293–322.

Meyer GM, Spay C, Laurencin C, Ballanger B, Sescousse G, Boulinguez P. Functional imaging studies of Impulse Control Disorders in Parkinson's disease need a stronger neurocognitive footing. Neurosci Biobehav Rev 2019; 98: 164–76.

Mosley PE, Paliwal S, Robinson K, Coyne T, Silburn P, Tittgemeyer M, et al. The structural connectivity of discrete networks underlies impulsivity and gambling in Parkinson's disease. Brain 2019; 142: 3917–35.

Nachev P, Kennard C, Husain M. Functional role of the supplementary and pre-supplementary motor areas. Nat Rev Neurosci 2008; 9: 856–69.

Nolte G, Ziehe A, Nikulin VV, Schlögl A, Krämer N, Brismar T, et al. Robustly estimating the flow direction of information in complex physical systems. Phys Rev Lett 2008; 100: 234101.

Pascual-Marqui RD. Standardized low-resolution brain electromagnetic tomography (sLORETA): technical details. Methods Find Exp Clin Pharmacol 2002; 24 Suppl D: 5–12.

Paz-Alonso PM, Navalpotro-Gomez I, Boddy P, Dacosta-Aguayo R, Delgado-Alvarado M, Quiroga-Varela A, et al. Functional inhibitory control dynamics in impulse control disorders in Parkinson's disease. Movement Disorders 2020; 35: 316–25.

Poldrack RA. Can cognitive processes be inferred from neuroimaging data? Trends Cogn Sci (Regul Ed) 2006; 10: 59–63.

Postuma RB, Berg D, Stern M, Poewe W, Olanow CW, Oertel W, et al. MDS clinical diagnostic criteria for Parkinson's disease. Mov Disord 2015; 30: 1591–601.

R Core Team. R: A language and environment for statistical computing. 2014

Rae CL, Nombela C, Rodríguez PV, Ye Z, Hughes LE, Jones PS, et al. Atomoxetine restores the response inhibition network in Parkinson's disease. Brain 2016; 139: 2235–48.

Ramoser H, Müller-Gerking J, Pfurtscheller G. Optimal spatial filtering of single trial EEG during imagined hand movement. IEEE Trans Rehabil Eng 2000; 8: 441–6.

Robbins TW, Arnsten AFT. The Neuropsychopharmacology of Fronto-Executive Function: Monoaminergic Modulation. Annu Rev Neurosci 2009; 32: 267–87.

Rubia K, Russell T, Overmeyer S, Brammer MJ, Bullmore ET, Sharma T, et al. Mapping motor inhibition: conjunctive brain activations across different versions of go/no-go and stop tasks. Neuroimage 2001; 13: 250–61.

Santangelo G, Raimo S, Cropano M, Vitale C, Barone P, Trojano L. Neural bases of impulse control disorders in Parkinson's disease: A systematic review and an ALE meta-analysis. Neurosci Biobehav Rev 2019; 107: 672–85.

Schoffelen J-M, Gross J. Source connectivity analysis with MEG and EEG. Human Brain Mapping 2009; 30: 1857–65.

Siri C, Cilia R, Reali E, Pozzi B, Cereda E, Colombo A, et al. Long-term cognitive follow-up of Parkinson's disease patients with impulse control disorders. Mov Disord 2015; 30: 696–704.

Spay C, Albares M, Lio G, Thobois S, Broussolle E, Lau B, et al. Clonidine modulates the activity of the subthalamic-supplementary motor loop: evidence from a pharmacological study combining DBS and EEG recordings in Parkinsonian patients. J Neurochem 2018; 146: 333–47.

Spay C, Meyer G, Lio G, Pezzoli G, Ballanger B, Cilia R, et al. Resting state oscillations suggest a motor component of Parkinson's Impulse Control Disorders. Clin Neurophysiol 2019; 130: 2065–75.

Sumner P, Nachev P, Morris P, Peters AM, Jackson SR, Kennard C, et al. Human Medial Frontal Cortex Mediates Unconscious Inhibition of Voluntary Action. Neuron 2007; 54: 697–711.

Sutherland MT, Tang AC. Reliable detection of bilateral activation in human primary somatosensory cortex by unilateral median nerve stimulation. Neuroimage 2006; 33: 1042–54.

Swick D, Ashley V, Turken U. Are the neural correlates of stopping and not going identical? Quantitative meta-analysis of two response inhibition tasks. Neuroimage 2011; 56: 1655–65.

Thibes RB, Novaes NP, Lucato LT, Campanholo KR, Melo LM, Leite CC, et al. Altered Functional Connectivity Between Precuneus and Motor Systems in Parkinson's Disease Patients. Brain Connect 2017; 7: 643–7.

Tichavsky P, Yeredor A. Fast Approximate Joint Diagonalization Incorporating Weight Matrices. IEEE Transactions on Signal Processing 2009; 57: 878–91.

Wardak C, Ramanoël S, Guipponi O, Boulinguez P, Ben Hamed S. Proactive inhibitory control varies with task context. Eur J Neurosci 2012; 36: 3568–79.

Weintraub D, Koester J, Potenza MN, Siderowf AD, Stacy M, Voon V, et al. Impulse Control Disorders in Parkinson Disease: A Cross-Sectional Study of 3090 Patients. Arch Neurol 2010; 67: 589–95.

Ye Z, Altena E, Nombela C, Housden CR, Maxwell H, Rittman T, et al. Selective serotonin reuptake inhibition modulates response inhibition in Parkinson's disease. Brain 2014; 137: 1145–55.

Yeredor A. Blind separation of Gaussian sources via second-order statistics with asymptotically optimal weighting. IEEE Signal Processing Letters 2000; 7: 197–200.

Zhang S, Li CR. Functional connectivity mapping of the human precuneus by resting state fMRI. Neuroimage 2012; 59: 3548–62.

Wiecki TV, Frank MJ. A computational model of inhibitory control in frontal cortex and basal ganglia. Psychol Rev 2013; 120: 329–55.

FIGURE LEGEND

Figure 1: Design and rationale. **A)** Illustration of the experimental design used to assess three different forms of inhibitory control with a Go/NoGo task. Participants were asked to react as fast as possible to a Go stimulus (diamond) by means of a button press, or to withhold the prepotent response to an equiprobable NoGo stimulus (X). **B)** The different possible forms of response inhibition have distinct dynamical signatures in the brain, accessible after spectral analysis at the source level. A tonic brain activity which occurs in anticipation of stimulation and desynchronizes after the presentation of a Go or NoGo signal is typical of proactive inhibitory control (contrast 1). Spectral activity specifically induced by NoGo stimuli (event-related synchronization) might be indicative of selective reactive inhibition (contrast 2). Spectral activity induced by a stimulus, whatever the stimulus, when the context is uncertain is likely to pinpoint non-selective reactive inhibition (contrast 3). Examples of power time-series in healthy participants are presented on a trial-by-trial basis (concatenated data sorted according to RT -black curve-, left side) and on a mean power basis (right side). All illustrations are adapted from (Criaud *et al.*, 2017) and (Albares *et al.*, 2015).

Figure 2: Data processing pipeline configuration (see text for details).

Figure 3: Global network involved in the inhibitory task. Illustration of various independent components (separated with gBSS and localized with sLoreta) and dynamical patterns (predicted by inhibitory models) within different frequency bands (β=beta; δ=delta; θ=theta). IC# is indicated in black square. An exhaustive list is presented in Table 2.

Figure 4: Neural correlates of motor impulsivity in PD patients with ICDs (ICDs+) with respect to PD patients without ICDs (ICDs-). Precuneus (ICs #4,6) and SMA (IC#8) beta activity (absolute power data averaged across subjects) is abnormal in ICDs+ patients. While ICDs- patients show a pattern of pre-stimulus activity suggesting increased proactive

inhibitory control when action restraint is required (increased power in Go trials) with respect to the control condition (Go_control trials), ICDs+ patients do not show similar activation. This dysfunction is associated with more commission errors and shorter RT in ICDs+ patients with respect to ICDs- patients.

Figure 5: Position of the dysfunctional sources within the functional fronto-parietal network. **A)** Stimulus-induced desynchronization of proactive activity (mean amplitude –Z-transformed- for each IC/Frequency band revealing consistent dynamics). Sources accounting for ICDs are highlighted in color. **B)** Lag statistics. The direction of functional connectivity was assessed by cross-correlation of instantaneous amplitudes. The directionality and delay between two sources were estimated by tracking significant increases of the lagged correlations in the post-stimulus period relative to spontaneous lagged correlations in the baseline. Only the significant results between the three sources accounting for differences between ICDs+ and ICDs- are displayed for illustrative purpose. **C)** Synthetic pattern of effective connectivity. The directionality, significance and delay between the three sources accounting for ICDs are indicated by arrows. The position of these major sources within the functional fronto-parietal network can be estimated by calculating the number of precedencies and subsequences (indicated by grey triangles) with respect to all other sources within the network.

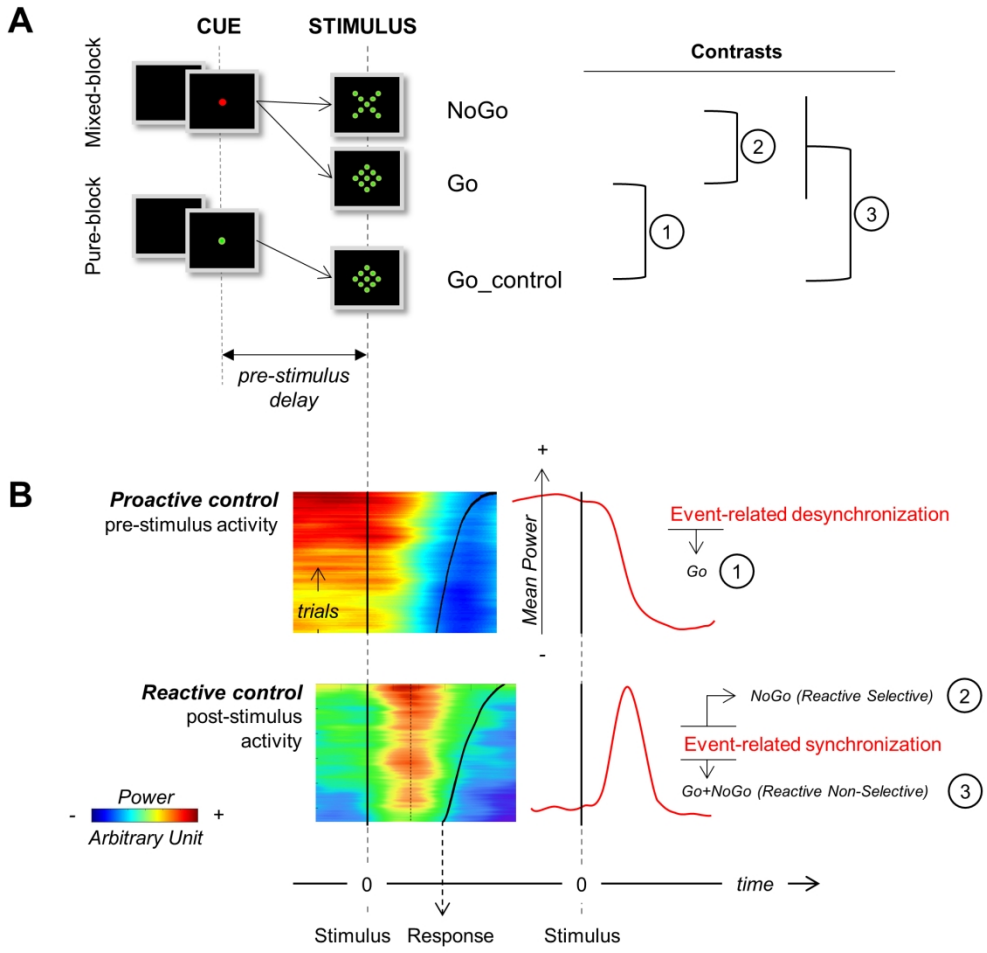

Design and rationale. A) Illustration of the experimental design used to assess three different forms of inhibitory control with a Go/NoGo task. Participants were asked to react as fast as possible to a Go stimulus (diamond) by means of a button press, or to withhold the prepotent response to an equiprobable NoGo stimulus (X). B) The different possible forms of response inhibition have distinct dynamical signatures in the brain, accessible after spectral analysis at the source level. A tonic brain activity which occurs in anticipation of stimulation and desynchronizes after the presentation of a Go or NoGo signal is typical of proactive inhibitory control (contrast 1). Spectral activity specifically induced by NoGo stimuli (event-related synchronization) might be indicative of selective reactive inhibition (contrast 2). Spectral activity induced by a stimulus, whatever the stimulus, when the context is uncertain is likely to pinpoint non-selective reactive inhibition (contrast 3). Examples of power time-series in healthy participants are presented on a trial-by-trial basis (concatenated data sorted according to RT -black curve-, left side) and on a mean power basis (right side). All illustrations are adapted from (Criaud et al., 2017) and (Albares et al., 2015).

180x180mm (300 x 300 DPI)

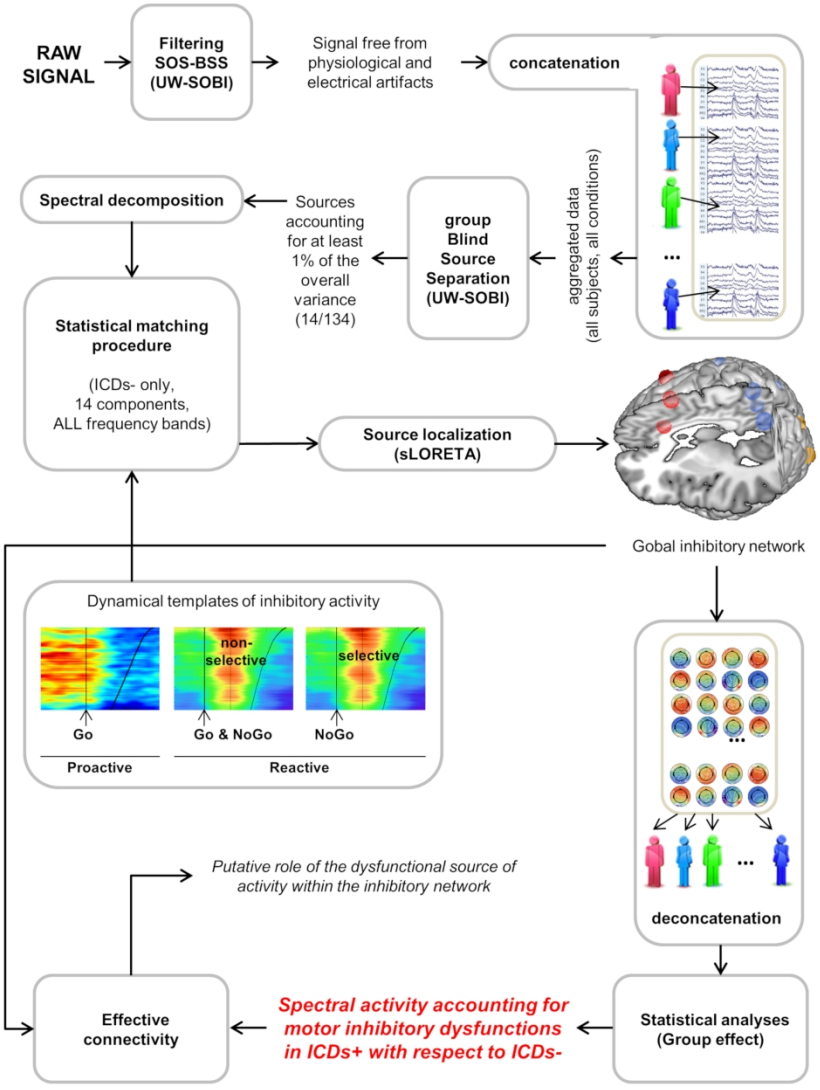

Data processing pipeline configuration (see text for details).

180x252mm (300 x 300 DPI)

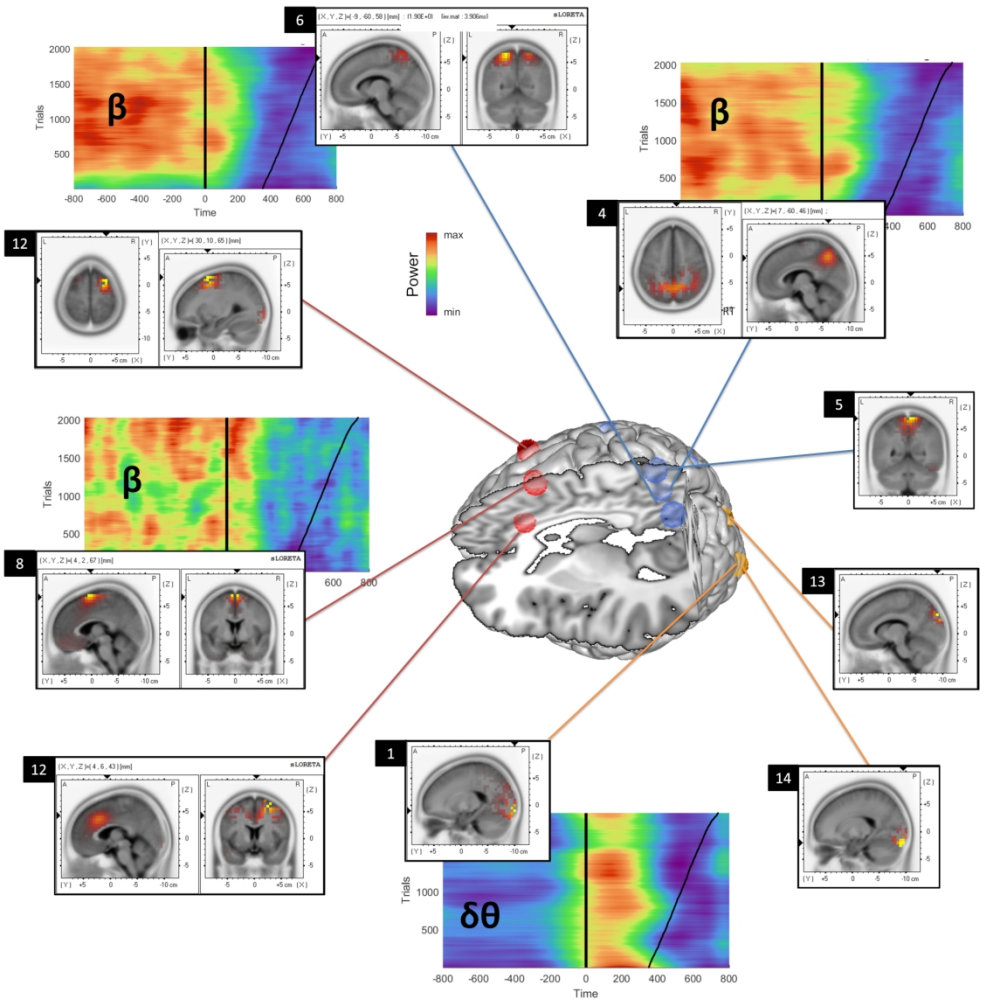

Global network involved in the inhibitory task. Illustration of various independent components (separated with gBSS and localized with sLoreta) and dynamical patterns (predicted by inhibitory models) within different frequency bands (β=beta; δ=delta; θ=theta). IC# is indicated in black square. An exhaustive list is presented in Table 2.

180x180mm (300 x 300 DPI)

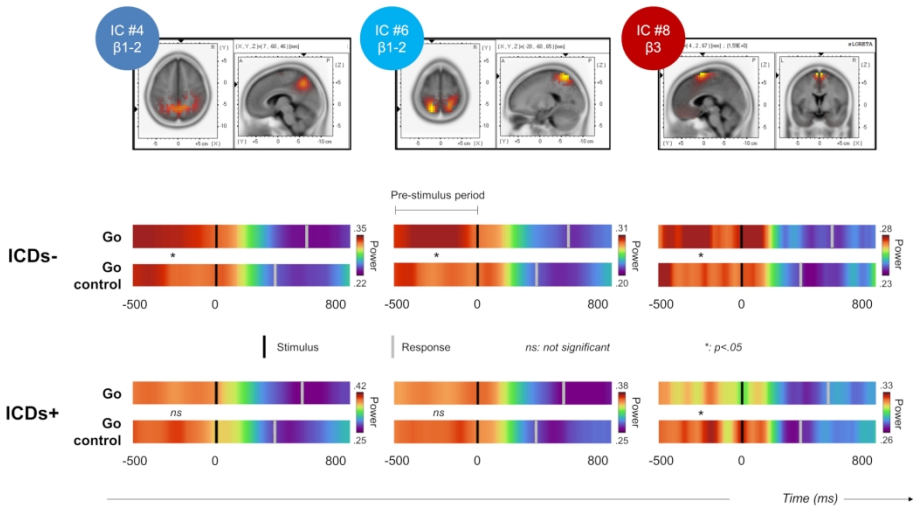

Neural correlates of motor impulsivity in PD patients with ICDs (ICDs+) with respect to PD patients without ICDs (ICDs-). Precuneus (ICs #4,6) and SMA (IC#8) beta activity (absolute power data averaged across subjects) is abnormal in ICDs+ patients. While ICDs- patients show a pattern of pre-stimulus activity suggesting increased proactive inhibitory control when action restraint is required (increased power in Go trials) with respect to the control condition (Go_control trials), ICDs+ patients do not show similar activation. This dysfunction is associated with more commission errors and shorter RT in ICDs+ patients with respect to ICDs- patients.

180x119mm (300 x 300 DPI)

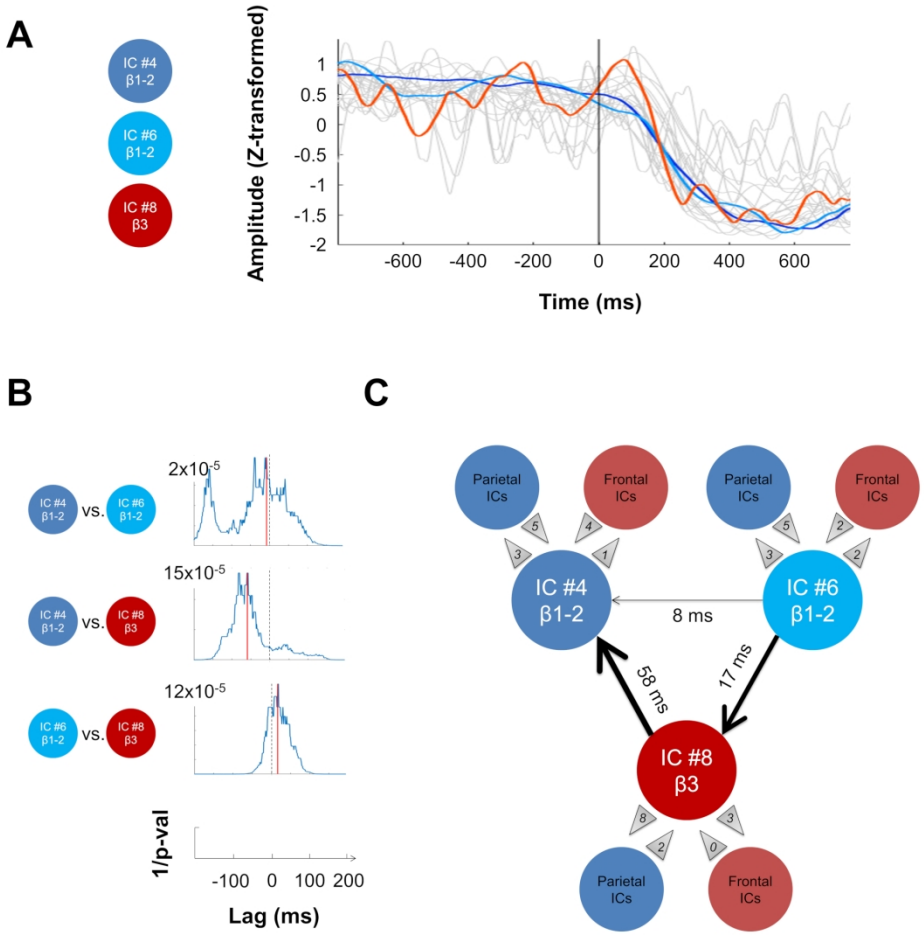

Position of the dysfunctional sources within the functional fronto-parietal network. A) Stimulus-induced desynchronization of proactive activity (mean amplitude –Z-transformed- for each IC/Frequency band revealing consistent dynamics). Sources accounting for ICDs are highlighted in color. B) Lag statistics. The direction of functional connectivity was assessed by cross-correlation of instantaneous amplitudes. The directionality and delay between two sources were estimated by tracking significant increases of the lagged correlations in the post-stimulus period relative to spontaneous lagged correlations in the baseline. Only the significant results between the three sources accounting for differences between ICDs+ and ICDs- are displayed for illustrative purpose. C) Synthetic pattern of effective connectivity. The directionality, significance and delay between the three sources accounting for ICDs are indicated by arrows. The position of these major sources within the functional fronto-parietal network can be estimated by calculating the number of precedencies and subsequences (indicated by grey triangles) with respect to all other sources within the network.

180x180mm (300 x 300 DPI)

Table 1: Patients characteristics.

	PD-ICDs+	PD-ICDs-	p-value
Demographics			
Number	22	19	-
Sex	21M / 1F	17M / 2F	-
Age	61.2 ± 7.0	58.4 ± 7.9	0.24
Disease duration	9.6 ± 4.8	7.8 ± 3.5	0.19
Clinical characteristics			
Total LEDD	791.6 ± 290.2	745.0 ± 205.8	0.56
Levodopa dose	621.7 ± 296.8	418.4 ± 208.8	0.016
DAAs dose (LEDD)	75.3 ± 87.4	254.4 ± 92.5	$1.1.10^{-7}$
Fluctuations	15 Yes / 7 No	5 Yes / 14 No	
H&Y stage	1.8 ± 0.7	1.6 ± 0.7	0.28
Predominant type, *type[number of patients]*	[AR]15 [TD]7	[AR]17 [TD]2	
UPDRS-III (ON)	11.8 ± 6.2	10.4 ± 7.8	0.51
Neuropsychological assessment			
MMSE	28.5 ± 1.3	29.4 ± 1.1	Cut-off > 26
FAB	15.5 ± 2.1	16.8 ± 1.2	Cut-off > 13.4
BDI	12.1 ± 8.4	7.5 ± 7.3	0.07
BIS-11	67.7 ± 13.6	63.8 ± 6.1	0.13
QUIP (A), *ICDs #[number of patients]*	[1]12; [2]7; [3]1; [4]2	*0*	-
QUIP (ABC), *ICDs #[number of patients]*	[1]9 ; [2]5 ; [3]6 ; [4]1 ; [5]1	*0*	-
A1 (Pathological gambling)	22	*0*	-
A2 (Hypersexuality)	7	*0*	-
A3 (Compulsive Buying)	3	*0*	-
A4 (Binge Eating)	5	*0*	-
B (Punding, Hobbyism or Walkabouts)	9	*0*	-
C (DDS)	0	*0*	-

Values are given as mean ± SD. ICDs= Impulse Control Disorders, Total LEDD= Total Levodopa Equivalent Daily Dose (mg/day), DAAs= dopamine agonists, H&Y= Hoeh & Yahr scale, AR=Akineto-rigid, TD=Tremor-dominant subtypes of PD patients, UPDRS-III= Unified Parkinson's Disease Rating Scale (part III), MMSE= Mini-Mental State Evaluation, FAB= Frontal Assessment Battery, BDI= Beck Depression Inventory, BIS= Barratt Impulsiveness Scale, QUIP= Questionnaire for Impulsive-Compulsive Disorders in Parkinson's Disease, ICBs= Impulsive-Compulsive Behaviors, DDS= Dopamine Dysregulation Syndrome.

Table 2: EEG results.

ICs explaining more than 1% of variance				Statistical matching procedure	Group analysis
#	Expl. var. (%)	sLORETA centroid coordinates (MNI, x y z)	Probability map extent Brodmann Areas	(significant frequency Bands)	(significant Group x Condition interactions)
1	15.9	-20 -100 -10	Lingual gyrus, Cuneus 17,18,19	Alpha	-
				Beta 1-2	-
				Beta 3	F(1,39)=5.20, p=.028 ICDs-: t=-1.73, p=.092 ICDs+: t=1.49 , p=.14
2	9.7	-5 -70 -5	Lingual gyrus 18	Alpha	-
				Beta 1-2	-
				Beta 3	-
3	6.0	15 -75 55	Superior parietal lobule, Precuneus 7	Alpha	-
				Beta 1-2	F(1,39)=5.45, p=.025 ICDs-: t=-1.02, p=.31 ICDs+: t=2.33, p=.025 (Ctrl>Mix)
				Beta 3	-
4	4.1	35 -35 65 (7 -58 47)	Post-central gyrus, Pre-central gyrus, Precuneus 2, 3, 6, 7	Alpha	-
				Beta 1-2	F(1,39)=11.52, p=.0016 ICDs-: t=-3.91, p=.0004 (Mix>Ctrl) ICDs+: t=.77, p=.44
				Beta 3	-
				Low gamma	-
5	3.7	5 -55 70	Post-central gyrus, Precuneus 5, 7	Alpha	-
				Beta 1-2	-
				Beta 3	-
6	3.1	-20 -60 65	Superior parietal lobule, Precuneus 7	Alpha	-
				Beta 1-2	F(1,39)=11.35, p=.0017 ICDs-: t=-2.79, p=.008 (Mix>Ctrl) ICDs+: t=1.95, p=.058 (trend Ctrl>mix)
				Beta 3	-

				Low gamma	-
7	2.6	20 -90 -25	Fusiform gyrus 18	Alpha	-
				Beta 1-2	-
				Beta 3	-
8	2.5	5 5 70	Superior frontal gyrus, Medial frontal gyrus 6	Alpha	-
				Beta 1-2	F(1,39)=4.53, p=.040 ICDs-: t=-1.53, p=.134 ICDs+: t=1.48, p=.147
				Beta 3	F(1,39)=17.34, p=.00017 ICDs-: t=-3.01, p=.005 (Mix>Ctrl) ICDs+: t=2.88, p=.006 (Ctrl>mix)
				Low gamma	-
9	2.3	-30 -90 -20	Inferior occipital gyrus, Fusiform gyrus 18, 19	Alpha	-
				Beta 1-2	-
				Beta 3	-
10	1.7	25 -90 -25	Fusiform gyrus, Inferior occipital gyrus, Medial frontal gyrus, Post-central gyrus 3,6,18	Alpha	-
				Beta 1-2	F(1,39)=4.35, p=.044 ICDs-: t=-1.23, p=.227 ICDs+: t=1.74, p=.089
				Beta 3	-
				Low gamma	-
11	1.6	-30 -95 15	Middle occipital gyrus 19	Alpha	-
				Beta 1-2	-
				Beta 3	-
12	1.5	30 10 65 (5 22 34)	Middle frontal gyrus, Anterior cingulate 6, 32	Alpha	-
				Beta 1-2	-
				Beta 3	-
				Low gamma	-
13	1.2	-10 -90 35	Cuneus, Middle occipital gyrus 18, 19	Alpha	-
				Beta 1-2	-
				Beta 3	-

14	1.2	20 -95 -20	Fusiform gyrus, Lingual gyrus, Inferior occipital gyrus 17, 18	Alpha	-
				Beta 1-2	-
				Beta 3	-

Meyer et al.

Inhibitory control dysfunction in Parkinsonian Impulse Control Disorders

Supplementary Table 1: Connectivity results.

From… / To…	IC #4 – Beta 1-2 Lag (ms) – p-value	IC #6 – Beta 1-2 Lag (ms) – p-value	IC #8 - Beta 3 Lag (ms) – p-value
IC #3 - Alpha	-24ms - <.0001	-6ms - <.0001	119ms - <.0001
IC #3 - Beta 1-2	-151ms - .0001	-73ms - .0004	74ms - <.0001
IC #3 - Beta 3	17ms - <.0001	71ms - .0006	-17ms - <.0001
IC #4 - Alpha	0ms - <.0001	0ms - <.0001	77ms - <.0001
IC #4 - Beta 1-2	-	8ms - <.0001	58ms - <.0001
IC #4 - Beta 3	-17ms - <.0001	28ms - <.0001	78ms - <.0001
IC #4 - Low gamma	n.s.	n.s	n.s.
IC #5 - Alpha	29ms - <.0001	-3ms - <.0001	83ms - <.0001
IC #5 - Beta 1-2	-85ms - <.0001	-96ms - <.0001	-67ms - <.0001
IC #5 - Beta 3	40ms - <.0001	60ms - .0001	79ms - <.0001
IC #6 - Alpha	0ms - <.0001	0ms - <.0001	69ms - <.0001
IC #6 - Beta 1-2	-8ms - <.0001	-	-17ms - <.0001
IC #6 - Beta 3	-16ms - <.0001	-7ms - <.0001	1ms - <.0001
IC #6 - Low gamma	n.s.	n.s.	n.s.
IC #8 - Alpha	91ms - <.0001	108ms - <.0001	93ms - <.0001
IC #8 - Beta 1-2	-63ms - .0005	n.s.	n.s.
IC #8 - Beta 3	-58ms - <.0001	17ms - <.0001	-
IC #8 - Low gamma	n.s.	n.s.	n.s.
IC #10 - Alpha	62ms - <.0001	70ms - <.0001	101ms - <.0001
IC #10 - Beta 1-2	n.s.	-119ms - .0002	-61ms - <.0001
IC #10 - Beta 3	23ms - <.0001	-81ms - <.0001	96ms - <.0001
IC #10 - Low gamma	n.s.	n.s.	n.s.
IC #12 - Alpha	-10ms - <.0001	2ms - <.0001	0ms - <.0001
IC #12 - Beta 1-2	-81ms - <.0001	-125ms - <.0001	65ms - <.0001
IC #12 - Beta 3	-199ms - <.0001	-1ms - <.0001	39ms - .0002
IC #12 - Low gamma	n.s.	n.s.	n.s.